Proceedings of the 12th International Conference on
Aluminium Alloys, September 5-9, 2010, Yokohama, Japan

pp. 1673-1678

The effects of Low Frequency Electromagnetic Field on Multi-physical Fields during the Start-up phase of DC Casting Process

Haitao Zhang[1,a], Jianzhong Cui[1], and Hiromi Nagaumi[2]

[1] Key Lab of Electromagnetic Processing of Materials, Ministry of Education, Northeastern University, Shenyang, Liaoning, 110004, China

[2] Department of Casting Technology, Suzhou Institute for Nonferrous Metals Research, Suzhou, Jiangsu, 215026, China

A comprehensive mathematical model has been developed to describe the interaction of the multiple physics fields during the start-up phase of the conventional DC casting and *LFEC* (low frequency electromagnetic casting) process. The model is based on a combination of the commercial finite element package ANSYS and the commercial finite volume package FLUENT, with the former for calculation of the electromagnetic field and stress-strain field and the latter for calculation of the magnetic driven fluid flow, heat transfer and solidification. Moreover, the model has been verified against the temperature measurements obtained from two 7XXX aluminum alloy billets of 200mm in diameter, during the conventional DC casting and LFEC processes, respectively. There was a good agreement between the calculated results and the measured results. Further, comparison of the calculated results of LFEC process with that of the conventional DC casting process indicated that velocity patterns, temperature profiles, the sump evolution and stress and plastic deformation are modified remarkably by the application of a low frequency electromagnetic field during the start-up phase of DC casting.

Keywords: *low frequency electromagnetic casting; DC casting; coupled modeling; temperature field; fluid flow; solidification, stress-strain field.*

1. Introduction

The semi-continuous Direct Chill (DC) casting process has been almost exclusively to produce aluminum billets during the past 60 years owing to its robust nature and relative simplicity. Nowadays, operators of DC casting machines are interested in reducing their production costs. One of the main cost drivers is the scrap rate and one of the more frequent defects generated in DC casting is hot tearing in the center of the billet.

There are two distinct stages in DC casting process [1, 2]. Stage I or the start-up, during which time the liquid pool profile and thermal field evolve with time; stage II or steady state, during time they remain essentially constant. Steady state operation is usually achieved within a cast length of 0.5-1m for a fully developed sump. From the standpoint of defects, the most critical stage of the DC casting process is the start-up phase. Therefore, optimization of this transient phase is the key to the production of defect free ingot. Some methods are used control this transient phase, such as varying the shape of bottom block[3, 4], casting speed, and water flow rates [5,6] during the start-up phase.

In this paper, a method referred as LFEC process [7,8] is used to control the start-up phase. LFEC process is based on the conventional DC casting, in which low frequency electromagnetic field is used to control the macro-physical fields in the casting process. Further, the macro-physical fields and the crack occurring in casting process are studied by the numerical and experimental methods.

2. Numerical modeling and experiment

2.1 Numerical modeling

In the paper, a coupled model is used to describe the interaction of the multiple macro-physical fields-electromagnetic fields, fluid flow, temperature field, solidification and stress-strain field during the start-up phase of the conventional DC casting and LFEC process of the billets of 200mm in diameter. Moreover, this detailed model can be found in reference [9].

In order to model the interaction of the multiple physical fields in the two processes, the model used in this paper is implemented by the commercial software package Ansys and Fluent. Further, this modeling procedure of DC casting and LFEC processes is: firstly, the electromagnetic field is calculated by Ansys and the Lorentz force is obtained simultaneously; then, the Lorentz is added to the conservation equation of momentum as the momentum source term during solving flow field which is coupled with temperature field and solidification and these physical filed are calculated by Fluent; lastly, the calculated temperature is inputted into Ansys to calculate the stress-strain field which is carried by Ansys. In addition, the process of the DC and LFEC is dynamic process, that is, the length of billet is varied with time, and so two numerical techniques are used in the procedure of calculation-the dynamic mesh in Fluent for the calculation of fluid flow, heat transfer and solidification and element birth and death in Ansys for the calculation of stress-strain field.

2.2 Experiments

Two new 7XXX aluminum alloy billets with diameter of 200mm were cast by LFEC process and conventional DC casting process at melt temperature 1003K, and casting speed 85mm/min, respectively. The electromagnetic field was applied by a 80 turns water-cooling copper coil surrounding the mold made of stainless steel. The current frequency in the coil is fixed at 25 Hz and the current intensity is 120A in the LFEC process. Moreover, the nominal composition of the experimental alloys is listed Table 1.

Table 1 Chemical composition (mass %) of the experimental super-high strength Al alloys.

Zn	Mg	Cu	Zr	Fe	Si	Al
9.82	2.39	2.25	0.142	0.12	0.08	Balanced

3. Results and discussion

3.1 The experimental verification of numerical model

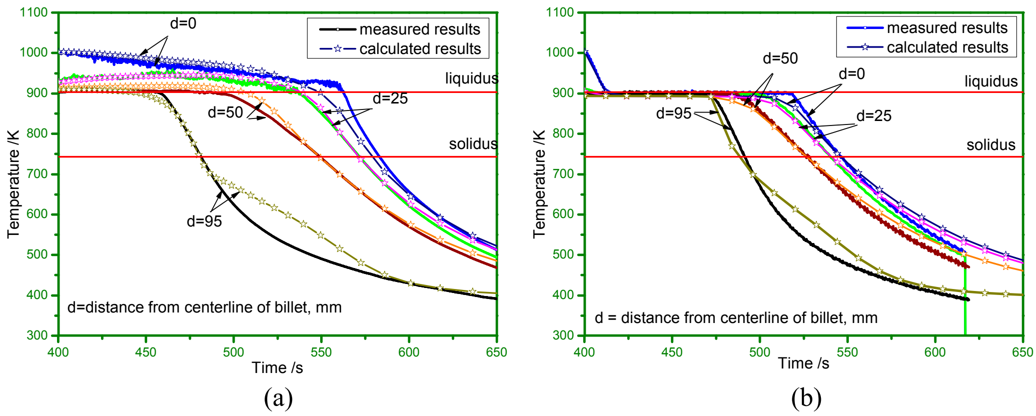

Fig. 1 Comparison between the calcualted and measured cooling curve in DC casting (a) and LFEC (b) processes

Fig. 1 (a) and (b) Show comparison of cooling curves for measurements and calculations at distance of 0mm, 25mm, 50mm and 95mm from the center of the billets cast during the conventional DC casting and LFEC processes, respectively. It is indicated that there is a good agreement between the calculated results and the measured results regardless of the conventional DC casting and LFEC processes.

3.2 The effect of electromagnetic field on fluid flow and heat transfer

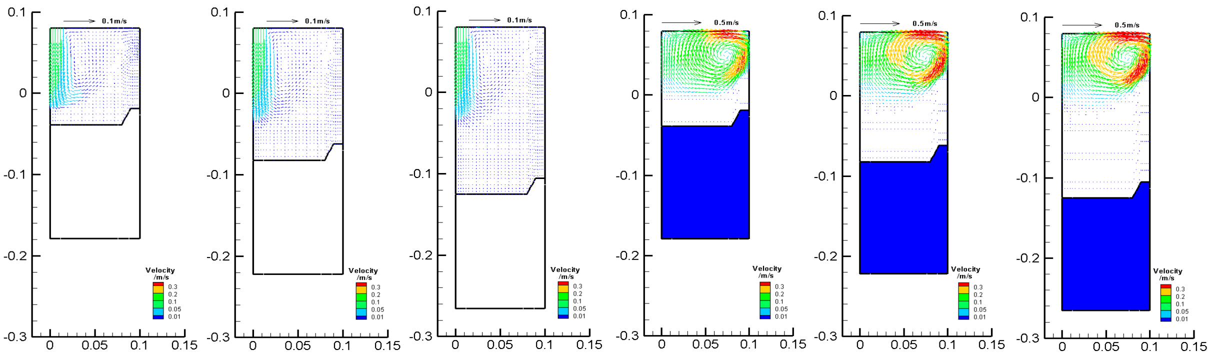

(a) (b) (c) (d) (e) (f)

Fig. 2 Velocity vectors at (a)40s,(b)70s,(c)100s in DC casting process and at (d)40s,(e)70s,(f)100s in LFEC process.

Fig. 2 (a)(b)(c) and (d)(e)(f) show the melt flow at 40s, 70s and 100s after the begin of casting in DC and LFEC processes, respectively. By comparison between (a)(b)(c) and (d)(e)(f), it is found that the melt flow is entirely modified in velocity magnitude and direction by electromagnetic field at the any time of casting process. When the electromagnetic field is applied in the semi-continuous casting process, the flow direction in the melt pool is reversed and a small circulation is produced near the solidification front at the center of the billet. In addition, compared to in the convection DC casting, the maximum velocity is increased about five times and its location is moved from the inlet region to the contact position between the melt and the mold. The phenomena are commonly explained by the forced convection resulted from the rotational component of the electromagnetic force. In addition, the flow direction does not vary with time in DC and LFEC process, but the flow magnitude less vary with time, as shown in Fig. 3. In this figure, it is observed that the maximum velocity is constant value in DC casting because the maximum velocity is the pouring velocity. Moreover, the maximum velocity increase gradually and hold a constant value when the steady-static condition is achieved, because the melt flow is constrained by the no fully evolved sump.

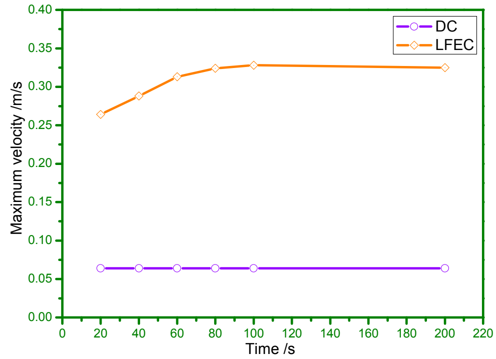

Fig. 3 The variation of maximum velocity with time.

Fig. 4 (a)(b)(c)and (d)(e)(f) shows the temperature profiles at 40s, 70s and 100s after the begin of casting in DC and LFEC processes, respectively. As seen from this figure, temperature distribution in the melt pool and the billets is modified remarkably in the total casting process when electromagnetic field is supplied. Firstly, it is observed that the temperature contours in Fig. 4 (d)(e)(f) are shifted upwards relative to Fig. 4 (a)(b)(c), which must result in the sump shape being entirely modified and the sump depth being remarkably reduced. In addition, compared to that in the absence of the electromagnetic field, the temperature in the bulk liquid is lower and more uniform in the presence of the electromagnetic field. The reason for the great modification of the temperature field is the vigorous forced convection induced by the electromagnetic stirring and that the heat flux along the longitudinal direction is increased due to the vigorous forced convection in the solidification front. As explained the reason in detail, in the conventional DC casting, the melt with high temperature reaches firstly the solidification front after the melt is poured into the melt pool from the inlet region, and then it is led to the contact region between the melt and the mold due to the thermal buoyancy, therefore, the sump depth is increased. In addition, because the flow velocity in the sump pool is very small, the heat transfer of the melt within the sump depend mainly on the conductive heat transfer, which results in uneven temperature distribution in the melt pool. However, in LFEC process, due to the electromagnetic field action, the melt with high temperature reaches firstly the contact region between the melt and the mold along the free surface and its temperature is decreased as soon as it is poured into the melt pool, and then the melt cooled by the mold reaches the solidification front, which must results in the temperature at the solidification front being decreased and the sump depth becoming very shallower. In addition, the heat transfer manner in the melt pool is mainly the conductive and convective heat transfer due to the vigorous forced convection induced by the electromagnetic stirring, therefore, the uniform temperature distribution within the sump is seen in Fig. 4 (d) (e) (f).

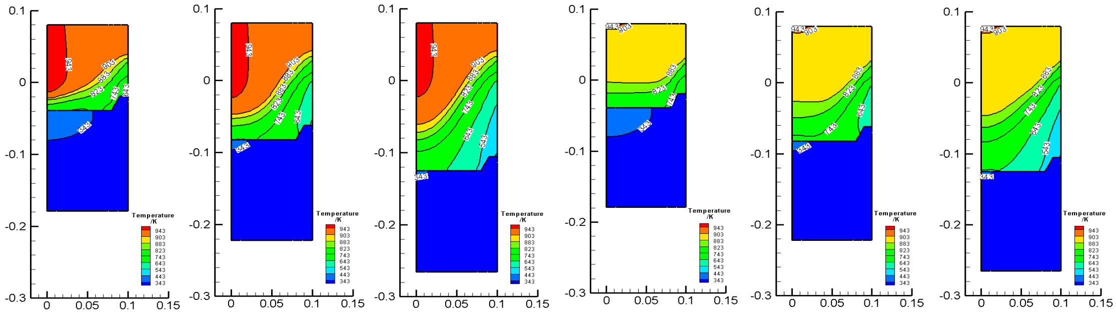

(a) (b) (c) (d) (e) (f)

Fig. 4 Temperature profile at (a)40s,(b)70s,(c)100s in DC casting process and at (d)40s,(e)70s,(f)100s in LFEC process.

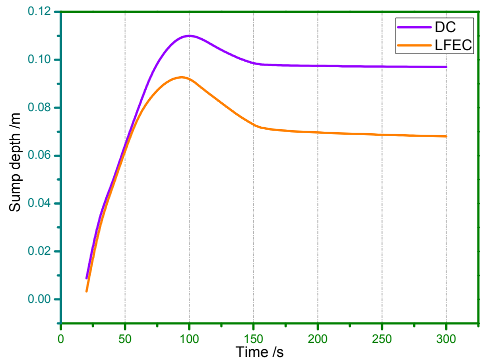

Fig. 5 The variation of sump depth with

Fig.5 shows the variation curve of sump with time. Regardless of DC casting and LFEC processes, it is found in this figure that sump depth increases firstly and then decreases to maintain a constant value finally. When the casting begins, the second cooling doesn't have effect on the center part of billet and cooling intensity of the base block is so smaller than that of second cooling, which results in the sump depth increasing with the increase of the billet length. The sump depth decreases when the second cooling has effect on the center part of billet after the casting begins to about 100s. Finally, the sump depth maintains constant when the steady static condition is gained. In addition, the sump depth in LFEC process is shallower than that in DC process, as illustrated in Fig. 5. It is reason that the temperature contours are shifted upwards in the present of electromagnetic field.

3.3 The effect of electromagnetic field on stress-strain field

The stress profiles in the billets at 120s,200s and 280s after the begin of casting in DC and LFEC processes are illustrated in Fig. 6 (a)(b)(c)and (d)(e)(f), respectively. From seen in the figure, the stress is increased with time because every part of billet constrains with each other induced by the increase of billet length. Moreover, the maximum stress migrates from the edge to the center of billet with the increase of the billet length, as illustrated in fig, which is because the cooling rate on the edge of billet is faster than that in the center of billet at first and then the cooling rate on the center overtakes that in the edge when the second cooling have entirely effect on the center part of billet. Fig. 7 (a)(b)(c)and (d)(e)(f) show the strain profiles in the billets at 120s,200s and 280s after the begin of casting in the DC and LFEC processes, respectively. The maximum strain appears on the center of billet during casting process. At the beginning of casting, the stress is smaller on the center of billet, but the resistance of deformation on this part is so smaller because of the higher temperature. Therefore, the bigger strain is generated on the center of billet though the generated stress is smaller. In addition, by comparison between in DC and LFEC process in Fig.7, it is found that the stress and strain generated in DC casting process is bigger than that in LFEC process, which results from the temperature field modified by applying electromagnetic field. Further, when electromagnetic field is applied in casting process, the temperature contours shifted upwards and the temperature difference is induced, which results in the cast stress and plastic strain reducing remarkably in the casting process.

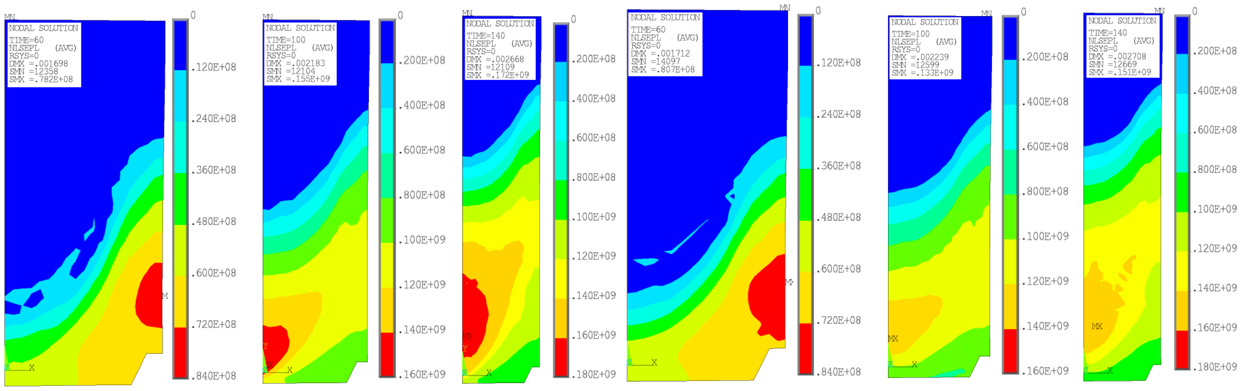

(a) (b) (c) (d) (e) (f)

Fig. 6 Equivalent plastic stress at 120s,200s and 280s in DC casting (a)(b)(c) and LFEC (d)(e)(f) processes.

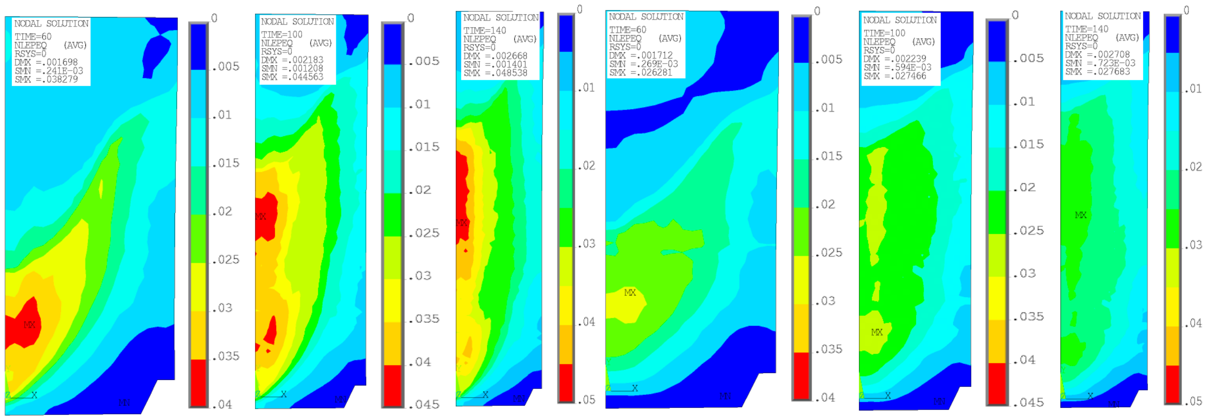

(b) (b) (c) (d) (e) (f)

Fig. 7 Equivalent plastic strain at 120s,200s and 280s in DC casting (a)(b)(c) and LFEC (d)(e)(f) processes.

3.4 The effect of electromagnetic field on crack

The photograph of DC and LFEC billets are shown in Fig8. it is found that the crack is formed in DC casting process, however, the billet without the crack defects is obtained in LFEC process. In order to study the crack occurring, the numerical method is used in this paper. Firstly, a criterion for crack occurring must be built. In this paper, a cracking damage index (CDI) and is as followed:

$$CDI = \varepsilon_{\theta} / \varepsilon_{f}$$

Where, ε_e and ε_f are the equivalent plastic strain and fracture strain at the different temperature, respectively. The crack can occur when CDI more than 1. Contrariwise, the crack can not occur.

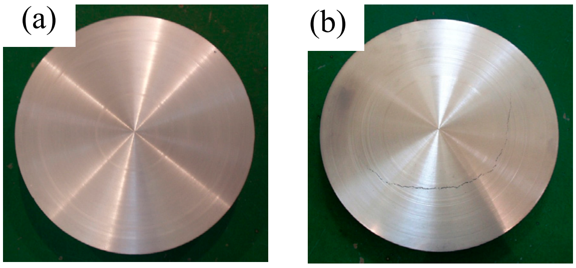

Fig.8 Photograph of DC and LFEC billets;(a) LFEC, (b) DC.

The coordinate, temperature and equivalent plastic strain at the time and location, when and where the maximum CDI (MCDI) generate in the DC casting and LFEC processes, is listed in table.2. Moreover, this time and location are called as the dangerous time and node, respectively.

Table. 2 Calculated results of MCDI

process	time	node	coordinate	temperature	Equivalent plastic strain	MCDI
DC	320s	1361	(0,0.35)	748.6162K	0.0313	1.29091
LFEC	290s	1269	(0.01688,0.355)	748.8022K	0.0201	0.82645

It is found in this table that the crack occurs in DC casting process and it does not in LFEC process based on the criterion used above.

4. Conclusion

In this paper, a comprehensive mathematical model has been developed to describe the interaction of the multiple physics fields during the start-up phase of the conventional DC casting and *LFEC* process. The model has been verified against the temperature measurements obtained from two 7XXX aluminum alloy billets of 200mm in diameter, in the conventional DC casting and LFEC processes, respectively. There was a good agreement between the calculated results and the measured results. Further, Comparison of the results for the macro-physical fields in LFEC process with that in the conventional DC casting process indicate the following characters at any time of casting process due to the application of electromagnetic field: a vigorous forced convection of the melt; an entirely changed direction of melt flow; a remarkably increased velocity of melt flow; a uniform distribution of temperature; a decreased gradient of temperature; the elevated isothermal lines; the reduced sump depth; the decreased stress and plastic deformation.

Acknowledge

This study was supported by the national “973” foundation of china (grant number: 2005CB623707). The authors are grateful to Dr. Ke, Qin, Yubo Zuo and Zhihao, Zhao for their help in the experiment.

Reference

[1] Wiskel, J.B., Ph.D Thesis, Dept. Of Metals & Material Engineering, University of British Columbia, Vancouver, Canada, 1996.
[2] Drezet, J.M., Ph.D Thesis, Dept. Of Metals, Ecole Polytechnique Federale de Lausanne, Lausanne, Switzerland, 1996.
[3] Schneider, W., and Jensen, E.K, Light Metal 1990, TMS(1990),pp. 931-936.
[4] Schneider, W., and Jensen, E.K, Light Metal 1995, TMS(1995),pp. 961-967.
[5] Yu, H., Light Metal 1980, TMS(1980),pp. 613-628.
[6] Bryson, N.B., U.S. Patent #3,411,079, 1969
[7] Jie Dong, Metallurgical and Materials Transactions A, Jan. 2005, pp 75-78.
[8] Jie Dong, Materials Letters, May. 2005, pp 1502-1506.
[9] Haitao Zhang, Hiromi Nagaumi, Yubo Zuo, Jianzhong Cui, Materials Science and Engineering A, Vol(448), MAR 15 2007, pp189-203.